Afyon Kocatepe Üniversitesi Uluslararası Mühendislik Teknolojileri ve Uygulamalı Bilimler Dergisi

Afyon Kocatepe University International Journal of Engineering Technology and Applied Sciences

AKÜ IJETAS Cilt 9**(1)** (2026) Haziran (42-58s) AKU IJETAS **Vol 9(1)** (2026) June (42-58pp)
DOI:10.53448/akuumubd.1923443

Araştırma Makalesi / Research Article
e-ISSN 2667-4165 (https://dergipark.org.tr/akuumubd)

Differential Diagnosis of Tuberculosis and Pneumonia in Cattle Lung Images Using Transfer Learning and YOLOv8: A Deep Learning Solution

Ali Çelik[1],*, İsmail Kırbaş[2], Özlem Özmen[3], Adem Milletsever[4]

[1] *Department of Physics, Burdur Mehmet Akif Ersoy University, Burdur, Turkey*
[2] *Department of Computer Engineering, Burdur Mehmet Akif Ersoy University, Burdur, Turkey*
[3] *Department of Pathology, Faculty of Veterinary Medicine, Burdur Mehmet Akif Ersoy University, Burdur, Turkey*
[4] *Department of Pathology, Faculty of Veterinary Medicine, Burdur Mehmet Akif Ersoy University, Burdur, Turkey*

e-mail: alicelik@mehmetakif.edu.tr ORCID ID: 0000-0001-8218-6512, ismailkirbas@mehmetakif.edu.tr ORCID ID: 0000-0002-1206-8294 , ozlemoz@mehmetakif.edu.tr ORCID ID: 0000-0002-5392-1626, amilletsever@mehmetakif.edu.tr ORCID ID: 0000-0002-3614-7798.
Geliş/Received : 05.04.2026 ; Kabul/Accepted : 08.05.2026 ; Revize/Revised : 02.05.2026

Keywords
Tuberculosis; Pneumonia; Machine Learning; Transfer Learning; YOLOv8

Abstract

Bovine tuberculosis (bTB) is a zoonotic, infectious, and chronic disease associated with significant economic losses, persisting as an endemic concern in various regions globally. Histopathological examinations are a crucial diagnostic method, particularly with the identification of Langhans giant cells, which serve as a distinctive marker. This study focuses on the differential diagnosis of tuberculosis from other types of pneumonia utilizing transfer learning. Additionally, it aims to enhance bTB diagnosis by employing the YOLOv8 algorithm to detect Langhans giant cells in histopathological images. While machine learning algorithms, such as logistic regression, SVM, and random forest, achieved a notable accuracy of 98.6% in the tuberculosis–pneumonia classification task, the YOLOv8 models demonstrated promising test-set performance in localizing Langhans giant cells, with mAP50 values ranging from 0.897 to 0.906. These findings offer a valuable contribution to the advancement of bTB diagnostic capabilities, particularly in distinguishing tuberculosis from other pulmonary conditions.

Sığır Akciğer Görüntülerinde Tüberküloz ve Pnömoninin Ayırıcı Tanısında Transfer Öğrenme ve YOLOv8: Derin Öğrenme Yaklaşımı

Anahtar Kelimeler
Tüberküloz; Pnömoni; Makine Öğrenmesi; Öğrenme Aktarımı; YOLOv8

Öz

Sığır tüberkülozu (bTB), zoonotik, bulaşıcı ve kronik bir hastalık olup, önemli ekonomik kayıplara yol açmakta ve dünyanın çeşitli bölgelerinde endemik bir sorun olarak varlığını sürdürmektedir. Histopatolojik incelemeler, özellikle ayırt edici bir belirteç olan Langhans dev hücrelerinin tanımlanmasıyla birlikte, tanıda kritik bir rol oynamaktadır. Bu çalışmada, transfer öğrenme yaklaşımı kullanılarak tüberkülozun diğer pnömoni türlerinden ayırt edilmesi ele alınmıştır. Ayrıca, histopatolojik görüntülerde Langhans dev hücrelerinin tespiti için YOLOv8 algoritması kullanılarak bTB tanısının geliştirilmesi amaçlanmıştır. Lojistik regresyon, SVM ve rastgele orman gibi makine öğrenmesi algoritmaları sınıflandırma görevlerinde %98,6 doğruluk oranına ulaşırken, YOLOv8 modelleri Langhans dev hücrelerinin lokalizasyonunda test seti üzerinde 0,897 ile 0,906 arasında değişen mAP50 değerleriyle başarılı performans göstermiştir. Elde edilen bulgular, özellikle tüberkülozun diğer akciğer hastalıklarından ayırt edilmesinde, bTB tanı yöntemlerinin geliştirilmesine önemli katkı sunmaktadır.

1. Introduction

Tuberculosis (TB) is caused by the Mycobacterium bacteria, which mainly affects the lungs but can also affect various body regions. Each year, TB-related mortality is significantly high due to diagnostic delays, incorrect diagnoses, and the lack of suitable remedies, all of which collectively contribute to a substantial number of fatalities (World Health Organization, 2020). Despite being a global challenge, the mortality rate is notably higher in low- and middle-income countries, as expected. Early diagnosis is, therefore, essential to halt the spread of the illness, achieve the best possible treatment results, and significantly lower death rates.

It is important to emphasize that tuberculosis poses a risk not only to human beings but also to cattle. Bovine tuberculosis (bTB), caused by Mycobacterium bovis (M. bovis), primarily affects cattle but also extends its impact to a diverse range of wild and domestic animals (O'Reilly and Daborn, 1995). While the transmission of TB in humans primarily occurs through the air, facilitated by activities such as sneezing or coughing, infected animals contribute to the spread of the disease through the ingestion of contaminated milk, water, or dairy products. Furthermore, transmission can occur through the inhalation of air contaminated with bacteria during the slaughtering process. However, pneumonia, an inflammatory condition mostly affecting the alveoli, may result from viral or bacterial infections to autoimmune diseases. In the specific case of bovine populations, pneumonia emerges as a prevalent respiratory affliction affecting cattle across all age groups. While many infectious agents, such as fungi, bacteria, and viruses, are the responsible for it, prominent bacterial contributors to bovine pneumonia include Histophilus somni, Mannheimia haemolytica, and Pasteurella multocida. Wheezing, nasal discharge, fever, and respiratory discomfort are examples of clinical symptoms in cattle. However, the occurrence of infection in cattle can be lessened by implementing preventive measures, including vaccination, appropriate ventilation, and limited exposure to infectious agents.

Machine learning algorithms have various applications in different domains, such as image recognition, speech recognition, classification, prediction, medical diagnosis, etc. (Celik and Sevli, 2022; Chan et al., 2020; Deng and Platt, 2014; Fujiyoshi et al., 2019; Ker et al., 2018; Noda et al., 2015; Shen et al., 2017; Wu and Chen, 2015). Particularly in the medical field, machine learning methods have demonstrated remarkable efficacy in enhancing the precision and overall quality of medical diagnoses. Many studies in the literature have been carried out to identify diseases like pneumonia or tuberculosis, highlighting the tremendous advancements in this field (Bangare et al., 2022; Becker et al., 2018; Bhartiya et al., 2021; Kant and Srivastava, 2018; Krishnamoorthy et al., 2022; Kumari et al., 2021; Kuo et al., 2019; Mollenhorst et al., 2019; More et al., 2021; Mwendo et al., 2023; Panicker et al., 2018; Patel et al., 2021; Pereira et al., 2020; Puttagunta and Ravi, 2021; Rahman et al., 2020; Stański et al., 2021; Venkataramana et al., 2022; Zak and Krzyżak, 2020). This collective effort not only propels innovative technologies forward but also significantly improves diagnostic capabilities in crucial medical scenarios.

The authors of the research paper (Patel et al., 2021) propose using three pre-trained convolutional neural networks (CNNs), namely VGG16, VGG19, and ResNet50, to classify chest X-ray images into normal or pneumonia cases. These CNNs are trained on a large dataset of natural images and can be fine-tuned for the pneumonia detection task using data augmentation techniques. The authors present accuracy, precision, recall, and F1-score for each model after evaluating performance on a dataset of 5,860 chest X-ray images. It is shown that VGG16 achieves the lowest loss of 0.09 and the best accuracy of 96.7%. VGG19 and ResNet50 follow with 95.6% and 88.14% accuracy and with a corresponding loss of 0.12 and 0.29, respectively. The authors conclude that transfer learning is an

effective and efficient method for pneumonia detection using chest X-ray images. They claim that their work can help medical practitioners and save many lives. They also suggest some future directions for improving the model performance and generalization.

Work (Venkataramana et al., 2022) presents a method for classifying chest X-ray images into different lung diseases using deep learning techniques. The main objective is to improve the accuracy and efficiency of diagnosis for tuberculosis, pneumonia, and COVID-19, which are common and severe respiratory infections. The paper proposes a multi-level classification model that first distinguishes tuberculosis and pneumonia and then classifies pneumonia into bacterial, viral, and COVID-19 types. The work additionally tackles the class imbalance issue in the datasets by employing data augmentation techniques to provide more synthetic examples for the minority classes. The study employs convolutional neural networks as the classifiers, feature selection, and autoencoders for an improvement in the accuracy of the model.

Artificial intelligence (AI) methods have multiplied our capabilities to extract quantitative information from digital histopathology images. AI is expected to reduce the workload for human experts, improve the objectivity and consistency of pathology reports, and have a clinical impact by extracting hidden information from routinely available data (Shmatko et al., 2022). The aim of this study is the detection of Langhans giant cells in histopathological preparations with AI methods.

The main contribution of this study is the development of a two-stage artificial intelligence framework for the differential diagnosis of bovine tuberculosis and pneumonia from histopathological lung images. In the first stage, discriminative features were extracted using a pre-trained ResNet-50 model and classified using conventional machine learning algorithms. In the second stage, YOLOv8-based object detection models were used to localize Langhans giant cells, which are diagnostically important histopathological indicators of bovine tuberculosis. By combining image-level classification with cellular-level localization, the proposed approach provides both diagnostic prediction and visual interpretability, thereby offering a supportive tool for veterinary pathology.

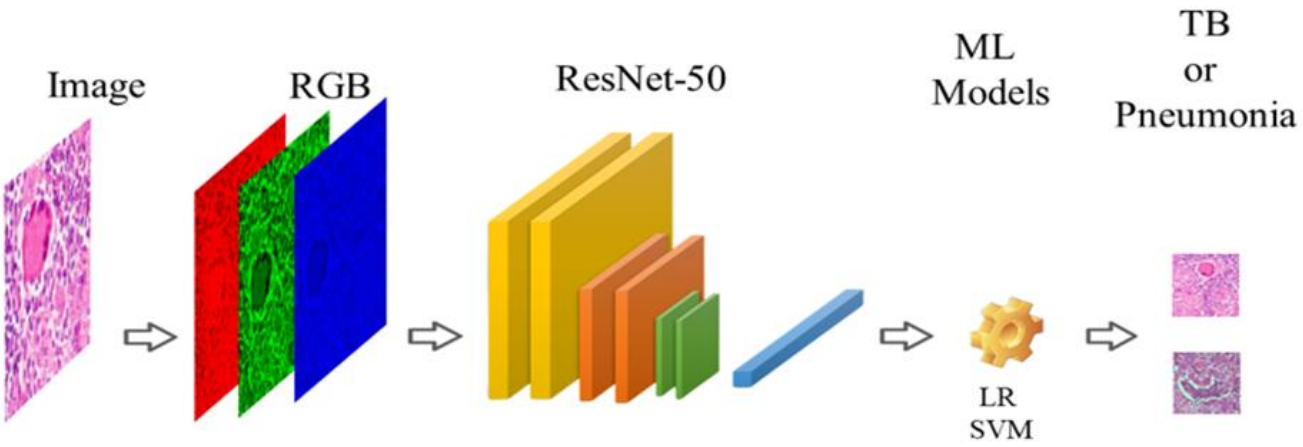

Figure 1. Schematic depiction of the transfer learning process

2. Methodology

The lung samples with typical tuberculosis lesions used in the study were obtained from a slaughterhouse where tuberculin-positive animals were subjected to compulsory slaughter (Suhut, Afyonkarahisar, Türkiye) and from the archives of the Department of Pathology. Microphotographs of lungs with pneumonia were taken from archive slides. Since tuberculosis is a notifiable disease, permission to collect the necessary materials for the study and approval from the ethics committee were obtained. The Local Ethical Committee on Animal

Research of Burdur Mehmet Akif Ersoy University/Türkiye approved the study (MAKU HADYEK /1177, dated 28.08.2023).

2.1 Histopathology Method

In this study, samples collected from the slaughterhouse were fixed in 10% formalin solution, routinely processed, and embedded in paraffin. Sections, each 5 microns thick, were extracted from both archived and freshly prepared blocks containing tuberculosis and pneumonia. The sections were stained with Hematoxylin-Eosin (HE). Microphotographs of pneumonia and characteristic tubercles were captured using the Database Manual CellSens Life Science Imaging Software System (Olympus Corporation, Tokyo, Japan).

2.2 Dataset

The dataset utilized in this study comprises microscopic images derived from cattle lung specimens, and its use is in strict compliance with the regulatory authorization issued by the Ministry of Agriculture and Forestry of the Turkish Republic. The primary objective of this research is to perform binary classification, specifically targeting the differentiation of pathological conditions, including pneumonia and tuberculosis, within the lung sections. Each of these two distinct classes, tuberculosis and pneumonia, consists of 247 and 256 image samples, respectively, in each category. All images in both classes have the same resolution of 3840 by 2027 in pixels.

The present study was designed to differentiate two pathological conditions, tuberculosis and pneumonia, using histopathological lung images. Therefore, only images from these two disease classes were included in the training, validation, and test sets. Healthy tissue images were not included as a separate class, since distinguishing healthy from diseased tissue was outside the scope of this work and could imply a three-class classification design. The focus was instead placed on distinguishing tuberculosis from pneumonia, which may present overlapping inflammatory and tissue-level features in histopathological sections.

2.3 Transfer Learning

Transfer learning, an essential machine learning component, has become a game-changing method in many fields (Bişkin et al., 2023; Celik, 2023). There exist two types of transfer of learning, one which is fine-tuning, and the other one is feature extraction. While the fine-tuning process requires fine-tuning of the parameters of the pre-trained model, the feature extraction technique, utilized in this work, extracts features from images in the new task using the pre-trained model. Subsequently, these extracted features are then utilized as inputs for the machine learning model for the specific task at hand. Schematic depiction of the transfer learning is illustrated in **Error! Reference source not found.**.

Transfer learning finds widespread application across domains. In computer vision, pre-trained convolutional neural networks (CNNs) have revolutionized image analysis tasks, such as image classification and object detection. In natural language processing, models like BERT have redefined the landscape by imparting contextual understanding to text, enriching sentiment analysis and text classification. The medical field witnesses the acceleration of diagnostic accuracy through transfer learning as models pre-trained on extensive medical image datasets expedite the development of radiology and pathology analysis tools. Ultimately, transfer learning is an indispensable tool, capable of propelling machine learning endeavors by efficiently transferring knowledge and expertise, and thus enabling models to achieve high performance with minimal data and computational resources.

2.4 ResNet-50

ResNet-50, or Residual Network-50, is a specialized convolutional neural network outlined in the influential 2015 paper (He et al., 2016). It distinguishes itself with a 50-layer structure, incorporating 48 convolutional layers, one MaxPool layer, and one average pool layer. What sets

ResNet-50 apart is its inventive architecture that integrates shortcut connections, allowing the model to effectively "skip over" certain layers. This unique approach addresses the vanishing gradient problem commonly encountered when incorporating numerous convolutional layers

2.5 Logistic Regression (LR)

Logistic regression, a statistical tool borrowed by machine learning, is a fundamental algorithm for classification tasks. It analyzes the probability of an instance belonging to a specific class, aiding decision-making. Unlike linear regression, which is prone to outliers, logistic regression uses the sigmoid function, represented by equation 1. Sigmoid function converts the best-fit line in linear regression into an S-shaped curve, which returns a value between 0 and 1.

$$\sigma(z) = \frac{1}{1 + e^{-z}} \qquad 1$$

Where z is referred to as the "logit", which is a linear combination of the input features (x_i) with associated weights (b_i) and can be represented as in equation 2.

$$z = b_0 + b_1 x_1 + b_2 x_2 + \cdots + b_n x_n \qquad 2$$

2.6 Support Vector Machines (SVM)

Support vector machines (SVMs), a type of machine learning algorithm developed by (Cortes and Vapnik, 1995), is capable of performing tasks such as classification, regression, and more. SVM is widely applied in various fields, some of which are image classification, spam detection, anomaly detection, glitch classification, and signal/background classification in particle physics. In binary classification scenarios, SVM works by finding the optimal hyperplane, which is a 1-D line separating the data points into different classes. In the case of more than two classes, the hyperplane is a two-dimensional plane or a more complex structure. While various hyperplanes might exist for classifying data, the SVM algorithm seeks to maximize the margin, which is the distance between the hyperplane and the nearest data points of each class, in order to improve the accuracy of the classification. SVM is not limited to linear problems; it can also handle nonlinear problems by employing kernel functions such as polynomial and sigmoid. These aforementioned kernel functions map data points into a higher-dimensional feature space, enabling a linearly separable or regressable in that space.

2.7 Random Forest

A supervised learning algorithm, Random Forest, is an ensemble learning algorithm and can be utilized for both the problem of classification and regression. It comprises a collection of decision trees, where each tree is constructed through bootstrapped subsets of the training data. To prevent overfitting, and improve generalization performance, only a random subset of the features is considered at each split in a tree. Instead of relying upon the outcome from a single tree, the algorithm takes predictions from multiple independent decision trees and provides a final output based on majority votes. Hence, Random Forest is known for its robustness and versatility and finds widespread application in various fields owing to its ability to deliver reliable predictions and valuable insights into features.

2.8 Naive Bayes

The Naive Bayes algorithm is a probabilistic classification technique based on Bayes' theorem (equation 3), which calculates the probability of an event given the probability of the observed event. The classifier assumes that each features have the same weight, and each pair of features is independent of each other given the class. Despite this simplifying assumption, Naive Bayes has demonstrated remarkable effectiveness in a variety of real-world applications. The algorithm is particularly very suitable for tasks such as text classification, spam filtering, natural language processing.

$$P(A \mid B) = \frac{P(B \mid A)P(A)}{P(B)} \quad 3$$

If the target variable represented in "y" and the feature vector in "X", which can be defined as $X = (x_1, x_2, \ldots\ldots, x_n)$, then Bayes' theorem can be applied to the data set in the following way:

$$P(y \mid X) = \frac{P(X \mid y)P(y)}{P(X)} \quad 4$$

In the case of naïve assumption, in which features are independent of each other, equation 4 could be re-written as the following by using the property A and B of being independent:

$$P(y \mid x_1, \ldots, x_n) = \frac{P(x_1 \mid y)P(x_2 \mid y) \ldots P(x_n \mid y)P(y)}{P(x_1)P(x_2) \ldots P(x_n)} \quad 5$$

Which then can be expressed in the following compact form:

$$P(y \mid x_1, \ldots, x_n) = \frac{P(y)\prod_{i=1}^{n} P(x_i \mid y)}{P(x_1)P(x_2) \ldots P(x_n)} \quad 6$$

The denominator part can be ignored as it is constant, and the maximum probability for the class 'y' can be obtained for the given set of features as following:

$$y = argmax P(y) \prod_{i=1}^{n} P(x_i \mid y) \quad 7$$

Where $P(y)$ target probability while $P(x_i \mid y)$ is conditional probability.

2.9 You Look Only Once (YOLO)

The Yolo algorithm, which was initially introduced in 2016, has been well-known and used widely for real-time object recognition and positioning in both images and videos since then. Besides being open-source, its high detection accuracy and fast processing have significantly contributed to its fame (Redmon et al., 2016).The YOLO object detection algorithm has undergone multiple versions, including YOLO, YOLOv2, YOLOv3, etc. Ultralytics, the developer of YOLOv5, has recently introduced YOLOv8, which exhibits notable improvements in both accuracy and speed compared to previous versions (Jocher et al., 2023). In addition, it has the capability to carry out classification, tracking, pose estimation, and segmentation activities in conjunction with object recognition. YOLOv8 incorporates multiple pre-trained models for different modes. For the classification mode, it utilizes datasets like ImageNet ("ImageNet Large Scale Visual Recognition Challenge | International Journal of Computer Vision," n.d.), which consists of more than 14 million images spanning 20,000 categories. Training of the models for detection, segmentation, and pose estimation is done using the COCO dataset (Lin et al., 2015), comprising 330,000 images and 80 classes.

In the present study, YOLOv8 was used for object-level localization of Langhans giant cells in histopathological images. Unlike image-level classification models, which assign a single label to the entire image, YOLOv8 produces bounding boxes around diagnostically relevant cellular regions. Therefore, its use in this study provides visual interpretability by indicating the locations of Langhans giant cells within tuberculosis tissue images.

There are five different pre-trained models, namely YOLOv8n, YOLOv8s, YOLOv8m, YOLOv8l, and YOLOv8x, for each of the three YOLOv8 model categories: detection, segmentation, and classification. All these five models are different from each other in terms of number of parameters. YOLOv8 nano stands out as the fastest and most compact, while YOLOv8 Extra Large (YOLOv8x) is relatively slower but performs better in terms of accuracy. YOLOv8 object detection and segmentation checkpoints are trained on the COCO

detection and segmentation dataset at a 640-pixel image resolution, respectively, while image classification models are trained on the ImageNet dataset with a resolution of 224 pixels.

Table 1. Hyperparameters which are optimized through GridSearch for both Logistic Regression, Support Vector Machines, Random Forest, and Naïve Bayes algorithms.

	ML Models			
Hyperparameters	SVM	LR	RF	Naïve Bayes
kernel	*linear*	-	-	-
C	*0.1*	-	-	-
Gamma	*1*	-	-	-
penalty	-	*l2*	-	-
solver	-	*liblinear*	-	-
n_estimators	-	-	*75*	-
max_depth	-	-	*10*	-
min_samples_split	-	-	*7*	-
min_samples_leaf	-	-	*2*	-
var_smoothing	-	-	-	*0.05*
priors	-	-	-	*None*

YOLO object detection has applications in many different fields, which makes it essential to many facets of our everyday life. Healthcare, agriculture, security surveillance, and autonomous vehicles are all domains in which it assumes a critical function. (Aldughayfiq et al., 2023; Ashraf et al., 2022; Benjumea et al., 2023; Lippi et al., 2021; Nguyen et al., 2019; Oguine et al., 2022; Paul et al., 2022; Qin et al., 2021). In healthcare, YOLOv3 aids in the real-time localization of organs during surgeries, which is particularly beneficial when dealing with biological diversity among patients. Notably, it has been employed for kidney recognition in CT scans, streamlining the process (Lemay, 2019). In agriculture, artificial intelligence and robotics have revolutionized the industry, with YOLO being a key component in vision-based harvesting robots. These robots replace manual labor, efficiently identifying different fruits and vegetables for harvest. Security surveillance extends beyond traditional use, as YOLOv3 was harnessed during the COVID-19 pandemic to estimate social distancing violations among individuals. YOLO's real-time object detection is also indispensable in the realm of self-driving cars. Autonomous vehicles rely on YOLO to accurately identify lanes, objects, and pedestrians, significantly enhancing road safety. The inherent real-time capabilities of YOLO make it a superior choice compared to simplistic image segmentation approaches, underscoring its critical role in shaping the future of autonomous transportation.

3. Proposed Method

Although YOLOv8 is capable of performing classification and detection tasks, a two-stage pipeline was preferred in this study because the two tasks address different diagnostic objectives. The ResNet-50-based feature extraction and machine learning classifiers were used for image-level differential diagnosis between tuberculosis and pneumonia. In contrast, YOLOv8 was used for object-level localization of Langhans giant cells, which provides visual interpretability and highlights diagnostically relevant cellular regions. Thus, the

YOLOv8 model complements the classification stage rather than replacing it. This structure enables the proposed framework to produce both a global disease classification and a localized cellular-level explanation.

The initial phase of this research encompasses data preprocessing and augmentation to prepare the dataset for analysis. The existing image dataset was split into training, validation, and test sets, at approximate ratio of 65%, 20%, and 15%, respectively. Specifically, train samples are distributed as 162 and 171 images for tuberculosis and pneumonia classes, respectively, while maintaining the test and validation sets of 35 and 50 samples for both classes. As the increase in the number of training set is more likely to improve the model's performance, data augmentation techniques were applied on the training data set. These augmentation techniques involved transformations such as rotation, horizontal and vertical flips, brightness and darkness adjustments, hue variations, and exposure manipulations. As a result of augmentation, we obtained 810 and 855 training images for tuberculosis and pneumonia classes, respectively. Since the classes are slightly imbalanced and thus, in order to balance the number of samples, we also employed random under-sampling method from scikit-learn library (Pedregosa, 2011). This method randomly selects a subset of images from the pneumonia class to match the number of images from the tuberculosis class. This ensures that none of the models being built are biased towards any class due to differences in the number of samples and learns the features of both diseases equally.

In the following phase of the study, the object detection model was trained for the localization of Langhans giant cells. For this purpose, tuberculosis histopathology images containing morphologically identifiable Langhans giant cells were used. The Langhans giant cells were manually annotated using the LabelImg software by veterinary pathologists Özlem Özmen and Adem Milletsever, who marked the relevant cellular regions with bounding boxes. Only clearly distinguishable Langhans giant cells were labeled in order to reduce annotation uncertainty. The annotated training images belonging to the tuberculosis class, generated through the augmentation of the initial training set of 162 images, were resized to 640 × 640 pixels, which is the input size used for YOLOv8 training. Using this annotated and augmented tuberculosis dataset, three pre-trained YOLOv8 models, namely YOLOv8m, YOLOv8l, and YOLOv8x, were trained for Langhans giant cell localization.

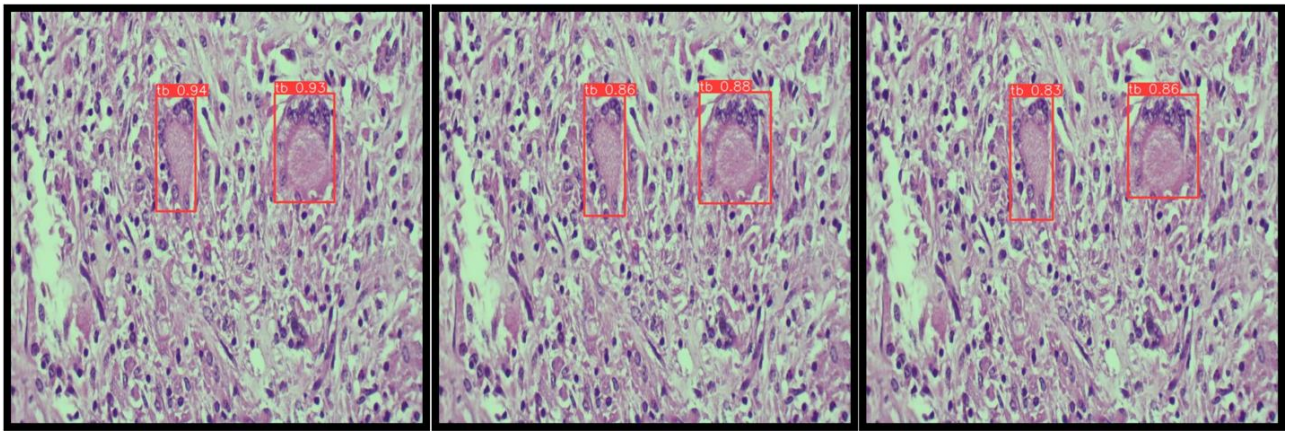

Figure 2. Three images with object detection confidence scores from three different pre-trained models, x-large, large, and medium, respectively.

Since the number of trainable parameters differs among the pre-trained YOLOv8 models, the performance of each model was assessed independently. The details of the trainable parameters for each pre-trained model are presented in Figure 3. During training, the maximum number of epochs was set to 200, and early stopping was implemented to reduce the risk of overfitting. Early stopping was triggered if no improvement was observed in the model performance for 30 consecutive epochs. For each YOLOv8 model, precision, recall, mAP50, and mAP50-95 were used as object detection performance metrics. The epoch-dependent performance curves of the models are shown in Figures 4, 5, and 6. A high recall

indicates the model's ability to capture relevant Langhans giant cell instances, whereas a high precision indicates reliable positive detections. The mAP50 metric evaluates detection performance at an IoU threshold of 0.50, while mAP50-95 provides a more stringent assessment by averaging performance across multiple IoU thresholds from 0.50 to 0.95.

Subsequently, attention was devoted to building binary classification models, which encompass multiple steps within themselves. In this phase of the work, resizing is applied to the training images, which are resized to the dimensions of 224 by 224. Following the aforementioned processes, images from both classes are then converted into the NumPy arrays and standardized using scikit-learn's standard scaler function, aligning them with a mean of zero and a standard deviation of one. These conversion processes are crucial for the feature extraction step. The standardized images are then pushed into the pre-trained ResNet-50 model for the purpose of extraction of informative and discriminative features. These extracted features are utilized as input for machine learning algorithms: Support vector machines, logistic regression, naïve bayes, and random forest. In order to ensure optimal performance for each model, we conducted parameter optimizations by exploring various combinations of hyperparameters. The optimal parameters for each model built are detailed in **Error! Reference source not found.**.

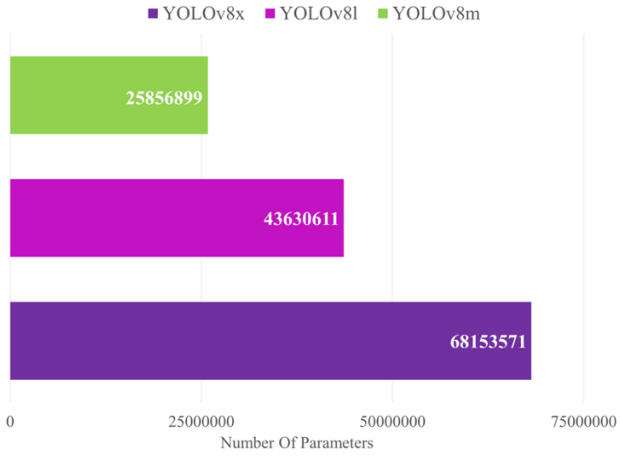

Figure 3. Parameter count of YOLOv8 pre-trained models.

After building four machine learning models, trained models are evaluated on the test set to check the performance of the models and classify tuberculosis and pneumonia classes. The performance metrics for the models are detailed in **Error! Reference source not found.**. The comprehensive depiction of the methodology is also presented in **Error! Reference source not found.**. Correctly identified images belonging to tuberculosis classes are subsequently pushed into models built for object identification using Yolov8. An example showcasing the performance of the three Yolov8 models is depicted in **Error! Reference source not found.**.

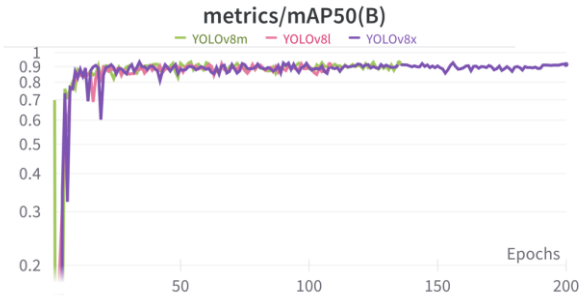

Figure 4. Distribution of mean Average Precision at IoU 0.50 (mAP50) for three YOLO models trained on the tuberculosis dataset. This metric provides an overview of the models' overall precision across varying confidence thresholds, emphasizing their effectiveness.

4. Results

The macroscopic examination of the lungs of slaughtered cattle at the abattoir revealed typical tubercles in the pleura and lung parenchyma, and samples were taken from these lesions (Figure 8).

Figure 5. Distribution of Recall values for three YOLO models trained on the tuberculosis dataset. Higher values indicate the models' ability to effectively capture relevant instances within the target classes.

When selecting areas containing Langhans giant cells from characteristic tubercles for tuberculosis microphotographs, areas without giant cells were chosen for lungs with pneumonia lesions. This was done with the aim of enabling artificial intelligence to identify Langhans giant cells.

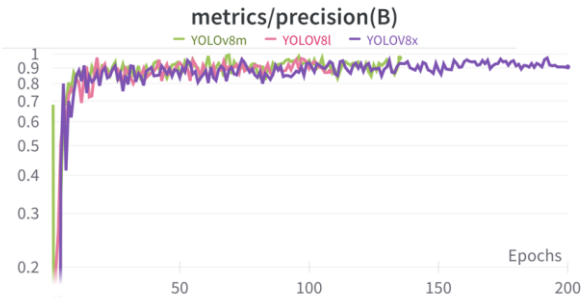

Figure 6. Precision distribution across confidence levels for three YOLO models trained on the tuberculosis dataset. Elevated precision values signify accurate positive predictions made by the models.

Following the development of binary classification models, their performance was rigorously assessed using the dedicated test set consisting of 35 images. While three out of four models demonstrated remarkable proficiency, achieving a 100% accuracy rate in the detection of tuberculosis cases, the model built with Naïve bayes has performed slightly lower than the others. The confusion matrix pertaining to the logistic regression model, accompanied by the corresponding Receiver Operating Characteristic (ROC) curve and its associated Area Under the Curve (AUC) value, is illustrated in **Error! Reference source not found.** and **Error! Reference source not found.**, respectively. These graphical representations offer valuable insights into the model's classification performance and its discriminative power.

Table 2. Performance metrics of models trained for classification of tuberculosis and pneumonia.

ML Models	Accuracy	Recall	Precision	F-1
SVM	0.986	1.000	0.972	0.986
LR	0.986	1.000	0.972	0.986
RF	0.986	1.000	0.972	0.986
Naïve Bayes	0.929	0.857	1.000	0.923

The performance of the binary classification models is evaluated based on accuracy, recall, precision, and F-1, and these metrics are detailed in **Error! Reference source not found.**. The images correctly identified as tuberculosis class were then subjected to another evaluation step: detection of Langhans giant cells. Three distinct YOLOv8 models, each of which had been trained with pre-trained models: YOLOv8x, YOLOv8l, and YOLOv8m, are utilized for the localizations. The qualitative detection examples are visualized in Figure 2, while the quantitative test-set performances of the YOLOv8 models are summarized in Table 3. Among the evaluated models, YOLOv8l achieved the highest precision value of 0.8951 and the highest mAP50 value of 0.9060, indicating strong detection performance at the IoU threshold of 0.50. YOLOv8x achieved the highest recall value of 0.8793, suggesting that it detected a larger proportion of true Langhans giant cell instances. The mAP50-95 values were comparable among the three models. Overall, these results show that all three YOLOv8 models provided promising localization performance for Langhans giant cells on the

independent test set. The relatively lower mAP50-95 values compared with mAP50 indicate that the models successfully detected Langhans giant cells at the IoU threshold of 0.50, while more precise bounding-box localization under stricter IoU thresholds remains a potential area for improvement.

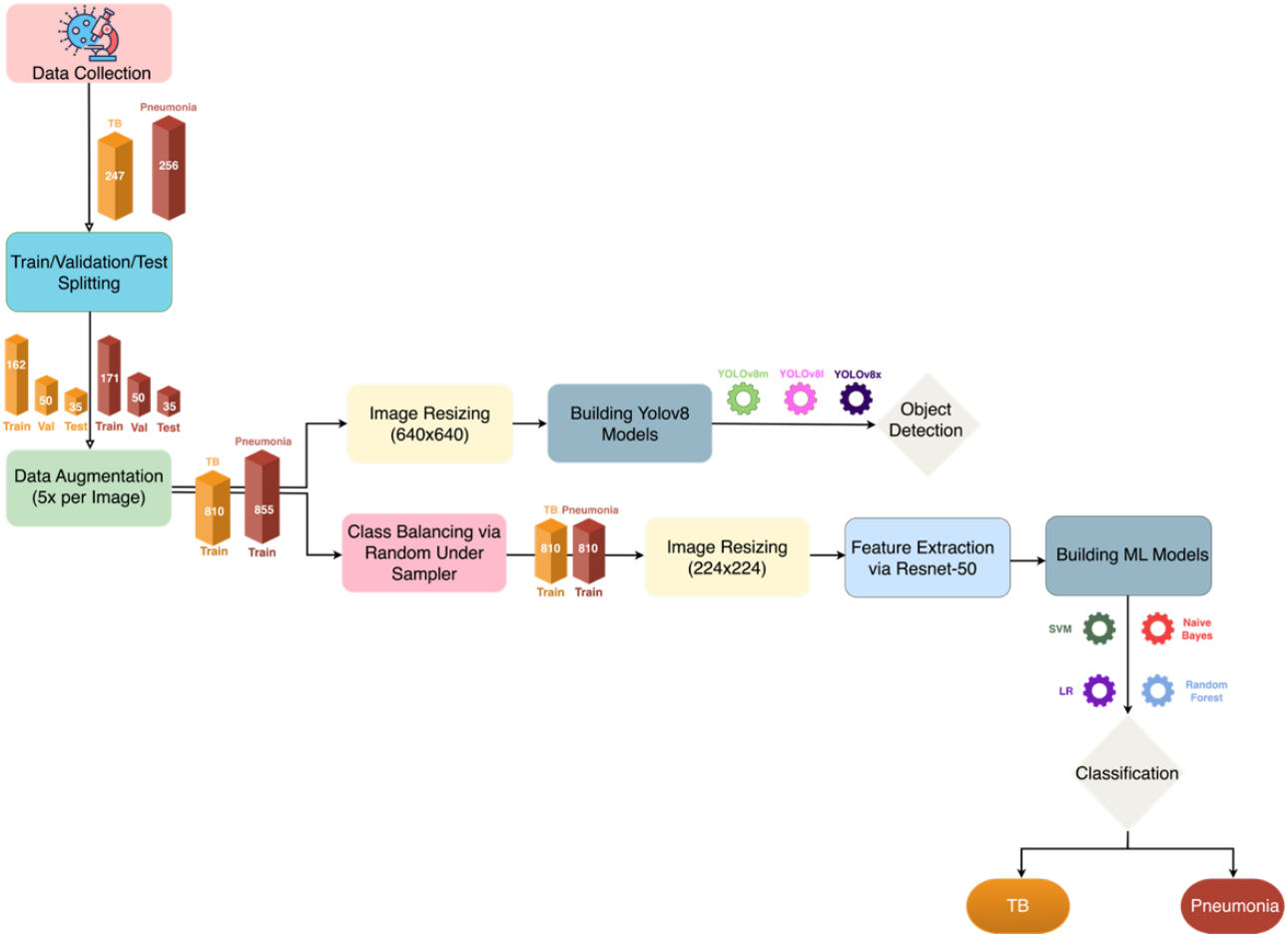

Figure 7. Schematic depiction of the methodology of the study.

Table 3. Test-set performance of YOLOv8 models for Langhans giant cell localization. Precision, recall, mAP50, and mAP50-95 values were calculated on the held-out test set using the best checkpoint of each model.

Model	Precision	Recall	mAP50	mAP50-95
YOLOv8m	0.861	0.857	0.897	0.593
YOLOv8l	0.895	0.810	0.906	0.584
YOLOv8x	0.871	0.879	0.901	0.592

5. Discussion

In this study, the aim was to differentiate tuberculosis from pneumonia in histopathological images of bTB and pneumonia-affected lungs using AI methods, and the AI was enabled to achieve this with a high accuracy rate.

For the early detection of bTB, a variety of antemortem and postmortem methods are employed; each has advantages and disadvantages in terms of diagnosis. While postmortem diagnosis relies on sufficient visual inspection, palpation, and further diagnostic processes like bacterial isolation, histopathology, and PCR to reach the final diagnosis, antemortem approaches rely either on cellular or humoral immune responses. Sequencing and bioinformatics tools such as type, mutation detection, phylogenetic analysis, molecular epidemiology, and interactions within the causal mycobacteria have recently become increasingly crucial for diagnosing bTB (Borham et al., 2022). This study investigated whether AI could discriminate between bTB and pneumonia in histopathological images and determined its potential to assist pathologists in this differentiation.

A key component of bTB control programs in endemic areas is postmortem analysis, which finds the infection in tuberculin test reactors or regularly slaughtered animals (Pascual-Linaza et al., 2017). The growth of granulomatous nodules known as tubercles, which are confined yellowish inflammatory nodules with a diameter of 2 to 20 mm, connective tissue encapsulating them, and frequently including core caseous necrosis and mineralization, is the hallmark of bovine tuberculosis (Domingo et al., 2014; Ozmen, 2009; Ozmen et al., 2005; Sevtekin and Ozmen, 2018). In this study, characteristic tubercles were diagnosed in slaughterhouse materials, and sampling was performed from these lesions.

The work (Sevtekin and Ozmen, 2018) described the distinctive histological images of tuberculous lesions, which were divided into four stages (stage I, II, III, and IV) according to microscopical classification. Stage I: Here are scattered lymphocytes, irregular epithelioid macrophages, and a few multinucleated giant cells of the Langhans type. Limited necrosis was seen in stage II granulomas, along with neutrophils, lymphocytes, and macrophages, as well as a small number of fibroblasts and Langhans-type cells. In the periphery of the core caseous necrosis, stage III granulomas showed Langhans-type large cells and epithelioid cells, together with central calcification. The inflammatory cell population near the fibrous capsule was made up of lymphocytes, neutrophils strewn throughout, and macrophages. The majority of Stage IV granulomas showed mineralization and necrosis. Thickly encapsulated lesions are indicative of less spread and a robust immune response against M. Bovis (Canal et al., 2017). Although not specific, Langhans giant cells are considered characteristic for the diagnosis of bTB (Borham et al., 2022; Canal et al., 2017; Ozmen, 2009; Ozmen et al., 2005; Sevtekin and Ozmen, 2018). Due to Langhans giant cells being characteristic cells observed in all stages of bTB, AI was trained to distinguish these cells in lesioned tissue. It was found that AI successfully accomplished this task, enabling the differentiation of bTB from other pneumonia lesions.

Figure 8. Goss appearance of lungs affected by bTB, which were collected for histopathological evaluations.

In a research paper that utilized chest X-ray images for identifying lung diseases (Rahman et al., 2020), limited datasets and deep learning models were employed. The process in this study comprised two stages: lung segmentation and disease classification. The U-net model was utilized for lung segmentation, extracting specific portions of the lungs from the images. Disease classification was performed using three pre-trained convolutional neural networks (VGG16, ResNet-50, and InceptionV3), fine-tuned on both segmented and non-segmented images. The research evaluated the method's performance on the Shenzhen Hospital and Montgomery datasets. The paper reported high accuracy and AUC scores for tuberculosis and pneumonia detection compared to existing solutions in the literature. For the pre-trained InceptionV3 model, AUC scores of 90%, 99%, and 93% were obtained for healthy, pneumonia, and tuberculosis classes, respectively.

In contrast to many studies focusing on X-ray images, this study has demonstrated how machine learning methods, utilizing transfer learning for feature extraction from microscopic photographs of bovine lung sections and subsequently employing YoloV8 for localizing Langhans cells, can distinguish between tuberculosis and pneumonia. The results of this study have indicated that AI can successfully

differentiate between bTB and pneumonia from histopathological images of bovine lungs with high success rates.

In the present study, the machine learning classifiers were optimized using GridSearch with 3-fold cross-validation, and the final performances of both the classification and YOLOv8-based localization models were evaluated on dedicated training, validation, and test sets. This strategy provided an independent test-set assessment of the proposed framework. Nevertheless, considering the limited number of histopathological images and manually annotated Langhans giant cells, future studies with larger and more diverse datasets may further benefit from 5-fold or 10-fold cross-validation to assess the robustness and generalizability of the models in greater detail.

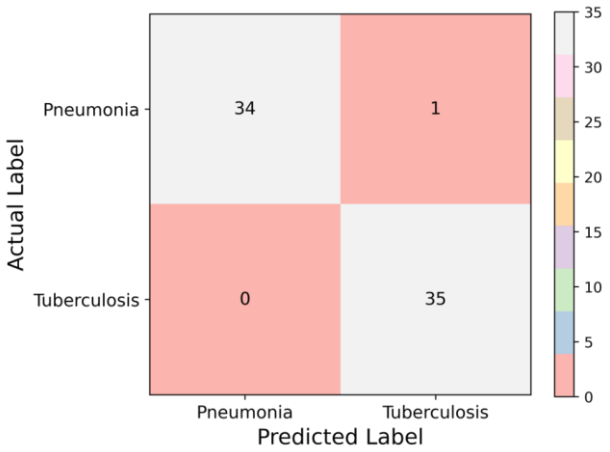

Figure 9. Confusion Matrix illustrating the performance of the logistic regression model in classifying tuberculosis and pneumonia classes. Notably, all tuberculosis instances are correctly identified, while one pneumonia instance is misclassified as tuberculosis.

6. Conclusion

The application of artificial intelligence across various fields is advancing rapidly, and veterinary medicine is no exception. Pathology, in particular, presents substantial potential for leveraging AI to improve disease diagnosis and differential diagnosis. This advancement holds promise for significantly assisting pathologists by enabling faster diagnostic assessments, thus offering valuable support in their work. As seen in human medicine, these developments in AI are beginning to influence veterinary pathology, contributing to the timely and accurate diagnosis of animal diseases.

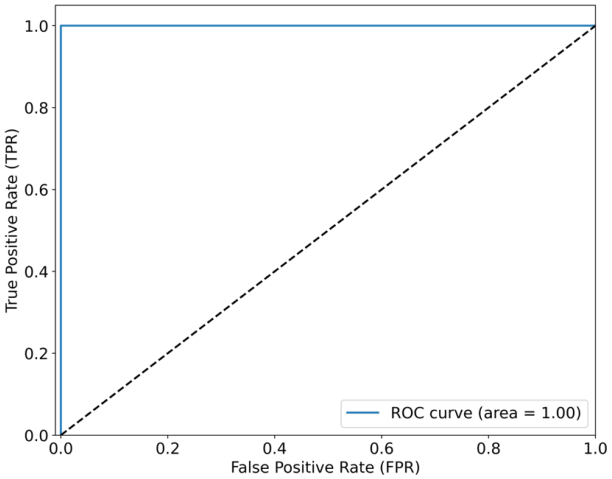

Figure 10. Receiver Operating Characteristic (ROC) Curve illustrating the performance of the logistic regression model in discriminating between tuberculosis and pneumonia classes.

The primary objective of this study was to assess the effectiveness of AI technologies, especially in diagnosing bovine tuberculosis and distinguishing it from other types of pneumonia in histopathological samples. By employing data preprocessing and augmentation techniques, the study achieved a balanced training dataset that represents tuberculosis and pneumonia classes evenly, which is crucial for accurate learning across both conditions. Using YOLOv8 models, the study localized Langhans giant cells in histopathological images with high precision, which is essential for differentiating tuberculosis from other respiratory conditions. Furthermore, high classification accuracy was obtained with binary classification models using ResNet-50-based feature extraction and various machine learning algorithms.

One distinguishing feature of this study is the use of tissue samples for tuberculosis and pneumonia classification, contrasting with the common reliance on chest X-rays in the literature. This approach allows for a deeper and more specific analysis of disease pathology at the tissue level, which can lead to more precise diagnoses. In addition, the localization of tuberculosis cells using YOLOv8 marks a significant innovation compared to general

diagnostic approaches, enhancing the accuracy of tuberculosis diagnosis by providing a detailed cellular-level analysis.

AI's integration into veterinary pathology is a transformative development that promises to reduce the workload for pathologists and improve diagnostic objectivity and accuracy, especially in cases where rapid decisions are critical. This technology will be especially valuable for early-career veterinary pathologists, offering a robust tool for developing their diagnostic skills. As AI continues to expand, its applications in veterinary pathology will also extend to veterinary training, offering students comprehensive and practical education that prepares them for professional practice.

Beyond diagnostic improvements, AI's role in veterinary pathology supports faster research and development, offering the potential to expedite the analysis of large datasets. This could lead to innovations in veterinary therapeutics, with new treatment protocols and optimized existing ones. Moreover, the cross-disciplinary collaboration among veterinarians, pathologists, computer scientists, and data analysts will further drive sophisticated AI solutions, shaping the future of veterinary practice and advancing animal health.

In summary, AI's integration into veterinary pathology is a revolutionary development that holds tremendous benefits for current and future veterinarians alike. This study has laid a solid foundation by illustrating AI's potential in diagnosing bTB and pneumonia in histopathological samples, paving the way for further research and applications. Expanding AI's role in veterinary pathology could lead to more comprehensive diagnostic and treatment methods across various animal species and diseases, ultimately fostering significant advancements in animal healthcare and veterinary medicine.

Acknowledgement

This study was supported by the Burdur Mehmet Akif Ersoy University Scientific Research Projects Commission. Project Number: 0895-YL-23.

Ethics Approval

The Local Ethical Committee on Animal Research of Burdur Mehmet Akif Ersoy University/Türkiye approved the study (MAKU HADYEK /1177, dated 28.08.2023).

References

Aldughayfiq, B., Ashfaq, F., Jhanjhi, N., Humayun, M., 2023. Yolo-based deep learning model for pressure ulcer detection and classification, in: Healthcare. MDPI, p. 1222.

Ashraf, A.H., Imran, M., Qahtani, A.M., Alsufyani, A., Almutiry, O., Mahmood, A., Attique, M., Habib, M., 2022. Weapons detection for security and video surveillance using cnn and YOLO-v5s. CMC-Comput. Mater. Contin 70, 2761–2775.

Bangare, S., Rajankar, H., Patil, P., Nakum, K., Paraskar, G., 2022. Pneumonia Detection and Classification using CNN and VGG16. International Journal of Advanced Research in Science, Communication and Technology 771–779. https://doi.org/10.48175/IJARSCT-3851

Becker, A.S., Blüthgen, C., Phi van, V.D., Sekaggya-Wiltshire, C., Castelnuovo, B., Kambugu, A., Fehr, J., Frauenfelder, T., 2018. Detection of tuberculosis patterns in digital photographs of chest X-ray images using Deep Learning: feasibility study. The International Journal of Tuberculosis and Lung Disease 22, 328–335. https://doi.org/10.5588/ijtld.17.0520

Benjumea, A., Teeti, I., Cuzzolin, F., Bradley, A., 2023. YOLO-Z: Improving small object detection in YOLOv5 for autonomous vehicles. https://doi.org/10.48550/arXiv.2112.11798

Bhartiya, P., Yadav, S., Gupta, A., Gupta, D., 2021. Pneumonia Detection Using CNN and ANN Based on Deep Learning Approach, in: Emerging Technologies for Healthcare. John Wiley & Sons, Ltd, pp. 181–201. https://doi.org/10.1002/9781119792345.ch7

Bişkin, O., Kırbaş, İ., Çelik, A., 2023. A fast and time-efficient glitch classification method: A deep learning-based visual feature extractor for

machine learning algorithms. Astronomy and Computing 42, 100683.

Borham, M., Oreiby, A., El-Gedawy, A., Hegazy, Y., Khalifa, H.O., Al-Gaabary, M., Matsumoto, T., 2022. Review on Bovine Tuberculosis: An Emerging Disease Associated with Multidrug-Resistant Mycobacterium Species. Pathogens 11, 715. https://doi.org/10.3390/pathogens11070715

Canal, A.M., Pezzone, N., Cataldi, A., Zumarraga, M., Larzabal, M., Garbaccio, S., Fernandez, A., Dominguez, L., Aranaz, A., Rodriguez-Bertos, A., 2017. Immunohistochemical detection of pro-inflammatory and anti-inflammatory cytokines in granulomas in cattle with natural Mycobacterium bovis infection. Research in veterinary science 110, 34–39.

Celik, A., 2023. A fast and time-efficient machine learning approach to dark matter searches in compressed mass scenario. The European Physical Journal C 83, 1150.

Celik, A., Sevli, O., 2022. Predicting Traffic Accident Severity Using Machine Learning Techniques. Türk Doğa Ve Fen Dergisi 11. https://doi.org/10.46810/tdfd.1136432

Chan, H.-P., Samala, R.K., Hadjiiski, L.M., Zhou, C., 2020. Deep Learning in Medical Image Analysis, in: Lee, G., Fujita, H. (Eds.), Deep Learning in Medical Image Analysis : Challenges and Applications, Advances in Experimental Medicine and Biology. Springer International Publishing, Cham, pp. 3–21. https://doi.org/10.1007/978-3-030-33128-3_1

Cortes, C., Vapnik, V., 1995. Support-vector networks. Mach Learn 20, 273–297. https://doi.org/10.1007/BF00994018

Deng, L., Platt, J., 2014. Ensemble Deep Learning for Speech Recognition. Presented at the Proc. Interspeech.

Domingo, M., Vidal, E., Marco, A., 2014. Pathology of bovine tuberculosis. Research in veterinary science 97, S20–S29.

Fujiyoshi, H., Hirakawa, T., Yamashita, T., 2019. Deep learning-based image recognition for autonomous driving. IATSS Research 43, 244–252. https://doi.org/10.1016/j.iatssr.2019.11.008

He, K., Zhang, X., Ren, S., Sun, J., 2016. Deep residual learning for image recognition, in: Proceedings of the IEEE Conference on Computer Vision and Pattern Recognition. pp. 770–778.

Jocher, G., Chaurasia, A., Qiu, J., 2023. YOLO by Ultralytics.

Kant, S., Srivastava, M.M., 2018. Towards automated tuberculosis detection using deep learning, in: 2018 IEEE Symposium Series on Computational Intelligence (SSCI). IEEE, pp. 1250–1253.

Ker, J., Wang, L., Rao, J., Lim, T., 2018. Deep Learning Applications in Medical Image Analysis. IEEE Access 6, 9375–9389. https://doi.org/10.1109/ACCESS.2017.2788044

Krishnamoorthy, N., Nirmaladevi, K., Kumaravel, T., Sanjay Nithish, K.S., Sarathkumar, S., Sarveshwaran, M., 2022. Diagnosis of Pneumonia Using Deep Learning Techniques, in: 2022 Second International Conference on Advances in Electrical, Computing, Communication and Sustainable Technologies (ICAECT). Presented at the 2022 Second International Conference on Advances in Electrical, Computing, Communication and Sustainable Technologies (ICAECT), pp. 1–5. https://doi.org/10.1109/ICAECT54875.2022.9807954

Kumari, L.V.R., Bokkolla, P., Syeeda, S.F., Gudala, S.P., Dasandla, M., 2021. Detection of pneumonia using Deep Learning, in: 2021 5th International Conference on Trends in Electronics and Informatics (ICOEI). Presented at the 2021 5th International Conference on Trends in Electronics and Informatics (ICOEI), pp. 1272–1279. https://doi.org/10.1109/ICOEI51242.2021.9452830

Kuo, K.M., Talley, P.C., Huang, C.H., Cheng, L.C., 2019. Predicting hospital-acquired

pneumonia among schizophrenic patients: a machine learning approach. BMC Medical Informatics and Decision Making 19, 42. https://doi.org/10.1186/s12911-019-0792-1

Lemay, A., 2019. Kidney recognition in ct using yolov3. arXiv preprint arXiv:1910.01268.

Lin, T.-Y., Maire, M., Belongie, S., Bourdev, L., Girshick, R., Hays, J., Perona, P., Ramanan, D., Zitnick, C.L., Dollár, P., 2015. Microsoft COCO: Common Objects in Context. https://doi.org/10.48550/arXiv.1405.0312

Lippi, M., Bonucci, N., Carpio, R.F., Contarini, M., Speranza, S., Gasparri, A., 2021. A yolo-based pest detection system for precision agriculture, in: 2021 29th Mediterranean Conference on Control and Automation (MED). IEEE, pp. 342–347.

Mollenhorst, H., Ducro, B.J., De Greef, K.H., Hulsegge, I., Kamphuis, C., 2019. Boosted trees to predict pneumonia, growth, and meat percentage of growing-finishing pigs1. J Anim Sci 97, 4152–4159. https://doi.org/10.1093/jas/skz274

More, K., Jawale, P., Bhattad, S., Upadhyay, J., 2021. Pneumonia Detection using Deep Learning, in: 2021 International Conference on Smart Generation Computing, Communication and Networking (SMART GENCON). Presented at the 2021 International Conference on Smart Generation Computing, Communication and Networking (SMART GENCON), pp. 1–5. https://doi.org/10.1109/SMARTGENCON51891.2021.9645844

Mwendo, I., Gikunda, K., Maina, A., 2023. Deep transfer learning for detecting Covid-19, Pneumonia and Tuberculosis using CXR images -- A Review. https://doi.org/10.48550/arXiv.2303.16754

Nguyen, Q.H., Nguyen, B.P., Dao, S.D., Unnikrishnan, B., Dhingra, R., Ravichandran, S.R., Satpathy, S., Raja, P.N., Chua, M.C.H., 2019. Deep Learning Models for Tuberculosis Detection from Chest X-ray Images, in: 2019 26th International Conference on Telecommunications (ICT). Presented at the 2019 26th International Conference on Telecommunications (ICT), IEEE, Hanoi, Vietnam, pp. 381–385. https://doi.org/10.1109/ICT.2019.8798798

Noda, K., Yamaguchi, Y., Nakadai, K., Okuno, H.G., Ogata, T., 2015. Audio-visual speech recognition using deep learning. Appl Intell 42, 722–737. https://doi.org/10.1007/s10489-014-0629-7

Oguine, K.J., Oguine, O.C., Bisallah, H.I., 2022. YOLO v3: Visual and Real-Time Object Detection Model for Smart Surveillance Systems (3s), in: 2022 5th Information Technology for Education and Development (ITED). IEEE, pp. 1–8.

O'Reilly, L.M., Daborn, C.J., 1995. The epidemiology of Mycobacterium bovis infections in animals and man: A review. Tubercle and Lung Disease 76, 1–46. https://doi.org/10.1016/0962-8479(95)90591-X

Ozmen, O., 2009. Immunohistochemical detection of C-reactive protein, serum Amyloid-A, caspase and Tumor Necrosis Factor-α in mediastinal lymph nodes in cattle with tuberculosis. Revue de Médecine Vétérinaire 160, 288–292.

Ozmen, O., Kurşun, O., Ozcelik, M., 2005. Bovine tuberculosis in Burdur, southern Turkey: epidemiological, pathological and economic study. The International Journal of Tuberculosis and Lung Disease 9, 1398–1402.

Panicker, R.O., Kalmady, K.S., Rajan, J., Sabu, M.K., 2018. Automatic detection of tuberculosis bacilli from microscopic sputum smear images using deep learning methods. Biocybernetics and Biomedical Engineering 38, 691–699. https://doi.org/10.1016/j.bbe.2018.05.007

Pascual-Linaza, A., Gordon, A., Stringer, L., Menzies, F., 2017. Efficiency of slaughterhouse surveillance for the detection of bovine tuberculosis in cattle in Northern Ireland. Epidemiology & Infection 145, 995–1005.

Patel, M., Sojitra, A., Patel, Z., Bohara, M.H., 2021. Pneumonia Detection Using Transfer Learning. International Journal of Engineering Research & Technology 10. https://doi.org/10.17577/IJERTV10IS100105

Paul, S., Ahad, D.M.T., Hasan, M.M., 2022. Brain Cancer Segmentation Using YOLOv5 Deep Neural Network.

Pedregosa, F., 2011. Scikit-learn: Machine learning in python Fabian. Journal of machine learning research 12, 2825.

Pereira, L.E.C., Ferraudo, A.S., Panosso, A.R., Carvalho, A.A.B., Mathias, L.A., Saches, A.C., Hellwig, K.S., Ancêncio, R.A., 2020. Machine Learning to predict tuberculosis in cattle from the state of Sao Paulo, Brazil. European Journal of Public Health 30, ckaa166.849. https://doi.org/10.1093/eurpub/ckaa166.849

Puttagunta, M.K., Ravi, S., 2021. Detection of Tuberculosis based on Deep Learning based methods. J. Phys.: Conf. Ser. 1767, 012004. https://doi.org/10.1088/1742-6596/1767/1/012004

Qin, Z., Wang, W., Dammer, K.-H., Guo, L., Cao, Z., 2021. Ag-YOLO: A real-time low-cost detector for precise spraying with case study of palms. Frontiers in Plant Science 12, 753603.

Rahman, T., Khandakar, A., Kadir, M.A., Islam, K.R., Islam, K.F., Mazhar, R., Hamid, T., Islam, M.T., Kashem, S., Mahbub, Z.B., Ayari, M.A., Chowdhury, M.E.H., 2020. Reliable Tuberculosis Detection Using Chest X-Ray With Deep Learning, Segmentation and Visualization. IEEE Access 8, 191586–191601. https://doi.org/10.1109/ACCESS.2020.3031384

Redmon, J., Divvala, S., Girshick, R., Farhadi, A., 2016. You Only Look Once: Unified, Real-Time Object Detection. https://doi.org/10.48550/arXiv.1506.02640

Sevtekin, M., Ozmen, O., 2018. Immunohistochemical examination of osteopontin and sirtuin-1 expression in cattle tuberculosis. Biotechnic & Histochemistry 93, 405–410.

Shen, D., Wu, G., Suk, H.-I., 2017. Deep Learning in Medical Image Analysis. Annual Review of Biomedical Engineering 19, 221–248. https://doi.org/10.1146/annurev-bioeng-071516-044442

Shmatko, A., Ghaffari Laleh, N., Gerstung, M., Kather, J.N., 2022. Artificial intelligence in histopathology: enhancing cancer research and clinical oncology. Nature cancer 3, 1026–1038.

Stański, K., Lycett, S., Porphyre, T., Bronsvoort, B.M. de C., 2021. Using machine learning improves predictions of herd-level bovine tuberculosis breakdowns in Great Britain. Sci Rep 11, 2208. https://doi.org/10.1038/s41598-021-81716-4

Venkataramana, L., Prasad, D.V.V., Saraswathi, S., Mithumary, C.M., Karthikeyan, R., Monika, N., 2022. Classification of COVID-19 from tuberculosis and pneumonia using deep learning techniques. Med Biol Eng Comput 60, 2681–2691. https://doi.org/10.1007/s11517-022-02632-x

World Health Organization, 2020. Global tuberculosis report 2020: executive summary. World Health Organization.

Wu, M., Chen, L., 2015. Image recognition based on deep learning, in: 2015 Chinese Automation Congress (CAC). Presented at the 2015 Chinese Automation Congress (CAC), pp. 542–546. https://doi.org/10.1109/CAC.2015.7382560

Zak, M., Krzyżak, A., 2020. Classification of lung diseases using deep learning models, in: International Conference on Computational Science. Springer, pp. 621–634.